Studying seriality in material culture by geometric morphometrics–gold wild boars from the Arzhan-2 barrow, Tuva

Fabrice Monna [a,*], Nicolas Navarro [b,c], Yury Esin [a], Tanguy Rolland [a], Josef Wilczek [d], Leonard Dumont [a,e], Jerome Magail [f], Anne-Caroline Allard [d], Carmela Chateau-Smith [b,g], Chechena Mongush [h], Saida Byrynnay [h], Paul Alibert [b]

[a] ARTEHIS, UMR, CNRS, 6298, Université de Bourgogne–Franche Comté, 6 boulevard Gabriel, Bat. Gabriel, Dijon, 21000, France
[b] Biogéosciences UMR CNRS 6282, Université de Bourgogne–Franche-Comté, 6 boulevard Gabriel, Bat. Gabriel, F-21000, Dijon, France
[c] EPHE, PSL University, 4-14 rue Ferrus, F-75014, Paris, France
[d] Centre André Chastel, UMR, CNRS, 8150, Faculté des Lettres Sorbonne Université, 2, rue Vivienne, Paris, 75002, France
[e] Ghent University, Department of Archaeology, Sint-Pietersnieuwstraat 35, 9000, Ghent, Belgium
[f] Musée D'anthropologie Préhistorique de Monaco, 56, boulevard du Jardin exotique, MC, 98000, Monaco
[g] CPTC, EA4178, Université de Bourgogne–Franche-Comté, 4 boulevard Gabriel, Dijon, 21000, France
[h] National Museum of the Republic of Tuva, 30 Titov Str, Kyzyl, 667000, Republic of Tuva, Russian Federation

ABSTRACT

In the field of material culture, seriality refers to the serial production of nearly the same object in terms of shape and size, yielding visually identical artefacts. Subtle variations may nevertheless occur, depending on the technologies used, or the number and reliability of moulds, for example. Geometric morphometrics based on landmark analysis, along with accompanying statistical techniques, provides methods well-suited for identifying small but archaeologically significant variations in shape and size within such datasets. In this study, we exemplify the efficiency of geometric morphometrics in a context of seriality, using a large series of centimetric-sized gold wild boars decorating a case for bow and arrows, discovered in the Arzhan-2 barrow of the early Scythian time. A total of twenty-seven 2D landmarks was collected for each specimen to assess the level of similarity between individuals with high precision, and to investigate the presence of subgroups, possibly indicating the use of several models. However, due to the homogeneous nature of the dataset, notable measurement errors may obscure the sought-after archaeological signal. To mitigate this, each specimen was measured twice by three different operators. Boas coordinates of the six replicates were then averaged, resulting in a reduction of the effect of measurement errors. Two distinct shape groups are identified, consisting of an approximately equal number of individuals. These findings suggest that the entire set of wild boars could have been produced *via* two separate manufacturing chains, possibly running in parallel, where two distinct, albeit very similar, solid models were involved. Within each group, discreet variations in size were observed. They are probably due to variable shrinkage during casting. These observations would have been difficult for the naked eye, even for an expert in the field, because the striking similarity within the series and the post-processing by the goldsmith obscure the shape signal originating from the moulds. Besides the original information provided here about the gold wild boars of Arzhan-2, it is worth emphasizing that the use of these techniques should be encouraged, particularly when applied to the study of seriality. The workflow described can easily be reproduced and adapted for almost any serially produced archaeological assemblage.

1. Introduction

In archaeology, serial production refers to objects produced as a series or belonging to a series. Seriality refers to another, more restrictive concept, involving the production of a large number of visually identical artefacts (Stockhammer, 2017). This type of production developed early in the third millennium BCE in the Near East, with the introduction of bronze casting (Stockhammer, 2017), and reached

---

* Corresponding author.
E-mail address: Fabrice.Monna@u-bourgogne.fr (F. Monna).

Europe in the Early Bronze Age at the beginning of the second millennium BCE (Sørensen, 2012; Johannsen, 2015; Gabillot et al., 2017). Over time, seriality flourished, with numerous technical innovations and the introduction of a broader array of raw materials. Seriality encompassed a great variety of artefacts, from common utilitarian objects, such as ceramics (e.g., Roberts, 1997), clay relief tiles (e.g., Fu, 2002), fibulae (e.g., Kruta, 1971), bronze weapons (e.g. Martinón-Torres et al., 2014), and palstaves (e.g., Webley and Adams, 2016), to more prestigious items made of precious metals (Liu et al., 2021), often produced in smaller quantities. The highest degree of resemblance was often sought for prestigious ornamental objects, especially when presented together as a set. The effect of repetition, particularly arranged in a geometric pattern, reinforces the sense of rhythm, quality, and abundance. To achieve this level of repeatability, several metalworking techniques were developed, such as openwork, lost-wax casting, and sheet-metal embossing (Armbruster, 2000; Minasyan, 2014, 2016; Ambruster and Meyer, 2024). More detailed research into the production of such sets should seek to identify the level of standardisation and specific aspects of the *chaine opératoire*. Grouping these nearly identical objects into series and even subseries may provide insights into craftspeople's habitus (Mauss, 1936; Bourdieu, 1977), and therefore into the economic structure of past communities, such as the organisation of labour, craft specialization, trade routes, and exchance networks (Rowlands, 1971; Costin, 1991; Costin, 2001; Bertemes and Furtwängler, 2008; Korol' and Naumova, 2017; Kuijpers, 2017). However, the identification of series within serially produced artefacts is a challenging task, as morphological variations are often too small to be identified with the naked eye, making fine typological classifications difficult or impossible. Other methods must therefore be used to identify groups, for example material analyses (Freestone et al., 2009; Martinón-Torres et al., 2014; Birch 2018) or geometric morphometrics (Wilczek et al., 2014, 2015; Birch and Martinón-Torres, 2019; Castiñeira-Latorre et al., 2024). This technique, used by biologists (e.g., Rohlf and Marcus, 1993; Adams et al., 2004, 2013; Mitteroecker and Schaefer, 2022), palaeontologists (e.g., Schaeffer, 2020; MacLeod, 2018), and archaeologists (e.g. Cardillo, 2010; Okumura and Araujo, 2019; Lundström et al., 2023; Pineda et al., 2023; Fernández Navarro et al., 2024; Jeanty et al., 2024), is specifically designed to quantify variation in form (a concept encompassing both size and shape). It is able to identify mathematically defined features to assess the level of similarity between items with a high degree of precision. Beyond the mathematical quantification of variation in both size and shape, this approach generates comprehensive visuals that enhance the interpretation of this complex issue (Klingenberg, 2013).

Our goal here is to demonstrate that geometric morphometrics can be highly effective in the context of seriality, to identify groups and possibly informative size variations. As a case-study, we apply this method to a set of very similar gold artefacts discovered in the Arzhan-2 barrow (Tuva Republic, Russian Federation), dating from the early Scythian period. Besides the two bodies buried in this tomb were 9000 artefacts, of which 5600 are of gold (total weight of gold ~20 kg; Parzinger, 2017). This collection has already been studied macro- and microscopically, to identify tool marks and other production-related features (Armbruster, 2009, 2017; Minasyan, 2004, 2014; Armbruster and Meyer, 2024). Metallographic, microwear, compositional, and isotopic analyses, among others, may also provide insights into the technology used and the potential origin of the raw materials (e.g., Pernicka, 2014; Leusch et al., 2014; for the origin of the raw materials used to craft the gold objects from Arzhan-2, see Zaykov et al., 2015). Here, we applied geometric morphometrics to a set of visually identical gold wild boars decorating a case for bow and arrows (gorytos) found in the barrow. In practice, a set of 2D landmarks, corresponding to homologous points (Bookstein, 1991; Webster and Sheets, 2010), was captured from the pictures of wild boars, placed to best describe the overall shape, while minimizing ambiguity about their position. This task is far from trivial, as these one-piece gold wild boars possess complex motifs,

smooth finishing, and post-casting work by the craftsman. Operator-induced measurement error during landmark digitalization may therefore contribute significantly to the observed variance, which from the intrinsic nature of seriality should be low. To address this issue, acquisition was performed by three operators, each of them duplicating landmark capture, to quantify both among-operator and digitalization errors. These sources of error were then reduced as much as possible. The potential presence of artefact subgroups was investigated, as such subgroups could indicate the use of several models to cast the objects. Conclusions are drawn regarding the causes of variation in form and the manufacturing processes involved.

Beyond the study of this specific set of gold wild boars, we provide guidelines for the use of geometric morphometrics in the broader context of seriality in material culture (where shape variations are expected to be very small), paying special attention to the statistical techniques that will allow the extraction of pertinent information from very similar objects. We also provide an extensively commented code and a set of functions to facilitate the reproduction and adaption of the workflow to almost any serially produced archaeological assemblage.

2. Material and methods

Corpus. One of the most remarkable exemplars of seriality in Protohistory is the multitude of gold zoomorphic artefacts discovered in the Arzhan-2 elite barrow, located in the Uyuk Valley, Tuva Republic (Fig. 1a). The princely tomb (grave n°5) constructed by nomadic populations in the 7th century BCE (Zaitseva et al., 2004) remained undisturbed until its excavation, from 2000 to 2004 (Chugunov et al., 2001, 2010, 2017). Within this tomb, among other artefacts, was a large number of nearly identical gold panther figures adorning the garments of each of the two bodies (2632 and 2297 respectively), with 244 large and 68 small gold wild boars in the form of decorative plaques for a gorytos. All these artefacts bear witness to great mastery of gold metalwork (see the reconstitution of the decorated costumes and equipment of the elite couple in Fig. 1b, and also Alexeyev, 2021, for an overview of Scythian gold artefacts). Currently, 50 of the 244 large gold wild boar plaques are curated by the State Hermitage Museum (St. Petersburg), while the remaining 194 are curated by the National Museum of the Republic of Tuva (Kyzyl). The obverse of the plaques is convex (Fig. 1c), and the reverse is concave; they measure approximately $2.5 \times 1.5 \times 0.4$ cm (Chugunov et al., 2010). On the reverse of the plaques are soldered ribbon-shaped eyelets, to attach them to the organic material tightly covering the gorytos (Fig. 1d, note that photographs of the reverse are available for only a few items). Among them, 111 individuals have three eyelets, while 133 have only two. This difference was used to construct two variants (Chugunov et al., 2010:44)

As a partial but well-documented 2D photographic record (including scale bar) of the large wild boars was available, this set was selected for analysis (Fig. 1c). Most of these items had already been photographed by the staff of the National Museum of the Republic of Tuva, using a Nikon D5200 DSLR equipped with a 45 mm lens (approximately 67 mm full-frame equivalency). During this step, the camera was maintained perpendicular to the main plane defined by the objects as much as possible to minimize optical distortion. All the 98 photographs of the boars with an inventory number in the state collection (i.e. #10517946 to #10518045, excluding #10518032, which has no scale), cropped and rescaled at 1200×1200 (resolution of ca. 0.03 mm/px), were downloaded from the State Catalogue of the Museum Fund of the Russian Federation (http://goskatalog.ru, no longer accessible in the EU since 2022). Twenty-eight photographs with no inventory number, at various resolutions, supposed to depict other items from the tomb, were also provided by the museum staff, forming an initial dataset of 126 individuals.

According to Minasyan (2004, 2014), the process of casting plaques involved the use of bi-valve clay moulds, created either from wax models or from pre-made objects. The initial step was to craft a model of the

Fig. 1. (a) Map of Asia, with the location of the Arzhan-2 site; (b) Reconstitution of costumes and equipment of the buried couple made by the experts of the Hermitage Museum. Picture from the Hermitage Museum (https://siberiantimes.com/science/casestudy/features/f0212-focus-on-tuva-stunning-treasures-and-macabre-slaughter-in-siberias-prehistoric-valley-of-the-kings/), the white arrow indicates the gorytos to which the gold wild boars were attached; (c) obverse and (d) reverse sides of one of the gold wild boars, photographed by the staff at the National Museum of the Republic of Tuva; on (c): the locations of the 27 landmarks; in red, the landmarks collected on the surface of the items, in white on their contour. (For interpretation of the references to colour in this figure legend, the reader is referred to the Web version of this article.)

intended plaque from wood, or more commonly from wax. This model was then used to create an impression in the obverse valve of the casting mould. Molten wax was poured into the mould, and excess wax was removed, leaving a thin convex-concave wax model, used to make the reverse clay valve. This bi-valve mould was then employed to cast the series. Armbruster (2010, 2017), and more recently Armbruster and Meyer (2024), have published a different description of the casting process. According to these authors, the plaques were cast using the lost-wax method. Wax models were mass-produced using a stone mould or the impression in clay of a solid model. They also suggested that items were not cast one by one but in lots, with several wax replicas connected to a wax rod as the central sprue. After casting, among other techniques, items could be finished with chisel and scraper, smoothed and polished, and poorly cast parts would be straightened.

Data acquisition. A set of 27 homologous landmarks to describe the artefacts was carefully selected to fulfil two main criteria: (*i*) comprehensively cover the entire morphology of the gold boar plaques, and (*ii*) be easily recognisable (Fig. 1c). In the field of biology, the second criterion corresponds to a discrete juxtaposition of tissues or defined by a single point without ambiguity, referred to as Type I landmarks according to Bookstein's classification (Bookstein, 1991). However, due to the nature of the target, in one piece, Type I landmarks could not be identified. Instead, Type II Bookstein landmarks, based on curvature characteristics, were therefore used throughout the study, despite being notoriously more challenging to acquire. A detailed investigation of measurement error was conducted to optimise measurement accuracy. This is a crucial step for objects that are very similar, such as the gold boars, where any morphological differences are expected to be slight.

The entire landmark configuration was therefore acquired by three different operators, each performing landmark acquisition twice, with a minimum of one week between sessions. This workflow ensured that each individual was digitized 6 times. Scale information was recorded simultaneously with the position of the 27 landmarks, using the scale bar depicted in all images (Fig. 1c). After completing the two data collection sessions, each operator thoroughly reviewed his own dataset, correcting landmark positions, if necessary, as operator practices may evolve over time. At this step, it became apparent that several individuals were illustrated by the same photograph in the state catalogue database (i.e. a single photo is repeated for items including # [1051]-7955, −7970, −7971, −7972, −7999, −8000, −8012, −8018, −8035, and −8040). In these cases, only one individual was kept per set. As a result, the dataset to be processed decreased from 126 to 107 individuals. From a statistical standpoint, although photographs of the entire set of individuals decorating the gorytos were unfortunately not available for analysis, a sample of approximately 50% of the total population (107 out of 244) provides sufficient representativity.

Geometric morphometrics. A partial generalised Procrustes analysis was first applied to the full set of scaled 2D landmark coordinates (Gower, 1975; Rohlf and Slice, 1990; Dryden and Mardia, 1998). After removing size by scaling the landmark configuration to unit centroid size, this procedure superimposes the landmark configuration on a common 2D space, using iterative processes of translation and rotation, based on least-square optimisation. This analysis decomposes the morphology of the items into two components: (*i*) a pure shape component, represented by Procrustes coordinates, and (*ii*) a size component, represented by the centroid size equal to the square root of the sum of the squared distances of each landmark from the centroid.

The orientation and translation transformations are not of particular interest here because they depend on the conditions in which the images were captured. In contrast, size is an important parameter since it is directly related to the production of the objects. For this reason, coordinates combining both size and shape information (Bookstein, 2021; Klingenberg, 2022) were preferred over Procrustes tangent coordinates, which focus only on the shape component of form. Several approaches have been proposed to produce size-and-shape spaces: (*i*) augmenting shape by the natural logarithm of the centroid size, resulting in the form space (Mitteroecker et al., 2004); (*ii*) suppressing the scaling step from the Procrustes superimposition, resulting in the conformation space (Dryden and Mardia, 1998; Klingenberg, 2022); (*iii*) unscaling the Procrustes-aligned coordinates, resulting in the Boas coordinate space (Bookstein, 2021). Approaches (*ii*) and (*iii*) resolve some of the problems associated with the size-and-shape space by providing consistent unscaled coordinates. They differ in approach: either considering size variation during the rotation step of the superimposition or using an unscaling step after the rotation step (Klingenberg, 2022). Here, Boas coordinates were chosen over conformation to ensure an alignment based on shape alone. In our context, variations in size are nonetheless small enough to provide similar results for all approaches. These Boas coordinates can be processed using Principal Component Analysis (PCA) to drastically reduce the dimensionality of the problem at hand (i.e. the number of landmarks × 2 (for X- and Y-coordinates) – 3). If the first two principal components (PCs) carry enough information, the shape and size of the individuals can be efficiently represented on a plane, resulting in a 2D morphospace with, in most cases, the first axis representing allometry, which is defined as the change in shape related to size (Klingenberg, 2022).

As all individuals were digitized by all three operators the same number of times, the experimental design is a balanced hierarchical repeated measurement. It can be modelled as a mixed model including two crossed factors: an operator term, considered as a fixed factor, and an individual term, considered as a random factor; each measurement is replicated twice (Nakagawa and Schielzeth, 2010; Liljequist et al., 2019). Setting the operator factor as fixed was chosen due to concerns that modelling a random effect variance with only three operators may

result in inappropriate generalization to the broader population of potential operators (Gomes, 2022). With this model, the total Procrustes variance can be partitioned into an "explained" component, corresponding to archaeologically meaningful shape variation (among-individual variation), and a "residual" component, which can be subdivided into intra-operator error (digitizing error) and inter-operator error. Within this framework, inter-operator error can advantageously be further decomposed into bias, i.e., a systematic error made by the operators (among-operator error), and a random effect, corresponding to the interaction between individuals and the operator factor, i.e., similar operator errors for the two replicates depending on the individuals. Note that, in the context of morphometric measurement errors, such a model is less frequently used than the nested model (Bailey and Byrnes, 1990; Yezerinac and al., 1992; Muñoz-Muñoz and Perpiñán, 2010). However, the latter collapses operator effects into a single component, preventing the separate assessment of systematic and random operator errors. With our balanced mixed model, variance components are obtained according to the expected mean squares of each term, with the among-individual variance, $\sigma_{ind}^2 = \frac{MS_{ind} - MS_{ind \times oper}}{n_{ind} \times n_{oper}}$, the among-operator variance $\sigma_{oper}^2 = \frac{MS_{oper} - MS_{ind \times oper}}{n_{ind} \times n_{rep}}$, and the random component of the operator variance, $\sigma_{ind \times oper}^2 = \frac{MS_{ind \times oper} - \sigma_e^2}{n_{rep}}$, where $\sigma_e^2 = MS_{residual}$ represents the residual variance, i.e., the digitization error. The term n_{rep} is the number of replicates, n_{oper} is the number of operators, and n_{ind} is the number of individuals. The systematic error made by the operator, the operator error related to the individual, and the digitizing error (%ME) were then computed as a proportion of their corresponding variance components (σ_{oper}^2, $\sigma_{ind \times oper}^2$, σ_e^2), in relation to the total variance, which is $\sigma_{total}^2 = \sigma_{ind}^2 + \sigma_{oper}^2 + \sigma_{ind \times oper}^2 + \sigma_e^2$. The two operator components can also be summed to provide the inter-operator error. Repeatability, R, was also computed as the intra-class correlation coefficient for consistency (Liljequist et al., 2019): $R = \sigma_{ind}^2 / (\sigma_{ind}^2 + \sigma_e^2)$, and reproducibility, R*, as the intra-class correlation coefficient for agreement: $R^* = \sigma_{ind}^2 / \sigma_{total}^2$.

The potential presence of multiple groups within the set of gold boars was investigated by applying multivariate Gaussian mixture models to the PCA scores (McLachlan and Peel, 2000). The aim of this modelling technique is to cluster individuals into *k* groups, in an unsupervised manner, using a probabilistic approach, with the assumption that a finite number of subpopulations are normally distributed and mixed to form the final dataset. For each group considered, the mean (μ), the covariance matrix (Σ), and the mixing probability (π) were optimally computed with an Expectation–Maximization algorithm (Dempster et al., 1977). Since the number of groups is a priori unknown, multiple cases with increasing *k* values were considered. The final model was selected using the Bayesian information criterion (BIC), which prevents overfitting, using penalisation when the number of parameters (groups) increases. Note that several options are possible regarding the modelling constraints applied on the covariance structure of the groups: e.g. spherical with equal volume, ellipsoidal with equal volume, etc. (Fraley and Raftery, 2006).

Practical implementation. Data acquisition was performed with the stereomorph library written for the R language, version 4.1.2 (https://www.r-project.org/, R Core Team, 2021). The code for data processing was produced with the geomorph (Adams and Otárola-Castillo, 2013) and mclust (Fraley and Raftery, 2006) libraries, combined with RStudio (https://posit.co/downloads/, RStudio Team, 2019). All software and packages used here are freely available. The images, along with all landmark coordinates and the code used for processing the data and generating the following figures and tests, are made available in a ZIP file as Supplementary Material SM1(https://search-data.ubfc.fr/FR-13002091000019-2024-05-27_Seriality-in-material-culture-by-Geometric.html, DOI:10.25666/dataubfc-2024-05-27).

3. Results and discussion

Landmark selection. Since each operator acquired the landmarks twice, it was possible to identify, for each operator, using a simplified version of the above explained model without operator and summing Procrustes variances across x-y coordinates of each landmark, the landmarks with the highest percentage of measurement errors (%ME) compared to the variation observed within the entire dataset. On average, the total %ME produced by the three operators accounted for between 13.9 and 16.5% of the total variance, corresponding to the sum of the among-individual variation plus the residual variation (Fig. 2). Interestingly, notable differences were observed at the scale of landmarks, since %ME ranged from less than 5% to more than 50% (Fig. 2). Despite prior agreement among the operators regarding the interpretation of images and placement of points, the relatively large differences in pattern observed between Fig. 2a, b, and 2c clearly illustrate the inconsistency inherent in personal interpretation by each operator. Indeed, identifying the precise position of tricky Type II landmarks may be somewhat subjective. Unsurprisingly, all three operators encountered difficulties with the same three landmarks (#16, #25, and #26). Note, however, that %ME calculation per landmark leads to an approximation because, with Procrustes registration, the position of each landmark depends to some extent on the position of all the others (Bookstein, 1991; Fruciano, 2016; Robinson and Terhune, 2017). Landmarks #16, #25, and #26 were therefore excluded from further analyses, so that computation was performed using only the remaining 24 more reliable landmarks. As a result, the total %ME by operator decreased to 11.7–14.2%. Although these values may seem relatively high, it is important to keep in mind that these percentages refer to minimum among-individual variations, which characterize the high-quality serial production of the gold boars.

Intra- and inter-operator errors. The PCA computed from the Boas coordinates of the six replicates (i.e. without landmarks #16, #25, and #26) is presented in Fig. 3. From the scree plot, the dataset appears to be mainly structured around the first two PCs, which account for 27.5% and 9% of the total variance (Fig. 3a), while from PC3 and beyond, the proportion of variance explained tends to taper off. This suggests that a projection on to the first two PCs may be sufficient for an initial exploratory analysis of the main drivers structuring the variance of the dataset (Fig. 3b), at least if genuine archaeological variations (e.g., presence of different moulds or progressive changes in the outputs of the fabrication pipeline) outweigh any random or systematic noise introduced by operators during acquisition or by post-casting work produced by craftsmen. If this is the case, the shape variations of interest should manifest primarily along the first few axes. At this step, it is informative to visually evaluate intra- and inter-operator errors by highlighting a few individuals chosen to cover the entire diagram (Fig. 3b). Based on the positions of these few examples, both types of errors (digitizing and among-operator) appear relatively small in comparison with among-individual variation. No clear preferential direction in the error components could be visually identified on the first two PCs of the total

variation (Fig. 3b), whether between the duplicates made by each operator, or between operators, suggesting that these errors do not correlate strongly with the main variation in form observed in the dataset. This result explains the high repeatability and reproducibility of the first two PCs, whereas the third PC presents a much lower level of reproducibility (Table 1). Overall, the values for intra- and inter-operator errors are very similar (12.1% and 11.3%, respectively). In other studies of this type, inter-operator error is often greater than digitization error (e.g. Wilson et al., 2011). This is not the case here: each operator may have lacked consistency during duplication because of the complexity of the dataset, but all operators followed the pre-defined guidelines for landmark digitization reasonably well. Consequently, only about half of the inter-operator error (6.2%) is related to systematic bias. As a result, reproducibility, R*, remains high when the measurements from the three operators are taken together (Table 1). Although intra- and inter-operator errors represent a similar amount of variance, the former appears to be isotropically distributed (Supplementary Material SM2a), indicating that this source of error is essentially random. Inter-operator error is more structured, with one major direction accounting for 43.6% of inter-operator variance (Supplementary Material SM2b). This result suggests that the positioning of at least a few of the landmarks was different for each operator. The main changes in form within the dataset corrected for measurement error can then be calculated from the among-individual variance component, σ^2_{ind}, and depicted as vector changes from the mean shape (Fig. 3c).

Clustering items and identifying size variations. As directional differences between operators remain acceptable, averaging replications should reduce the residual variance of the problem at hand, and hence improve the statistical power of further analyses by lowering the Type II error rate. All six measurements were therefore combined, and the resulting Boas coordinates of the individuals were projected on to the PCs of the among-individual variance, σ^2_{ind}, the first two increasing notably, and now accounting for 34.3% and 10.6% of the total variance (Fig. 4a).

A set of Gaussian mixture models was then applied, with different covariance structures for the groups, increasing the number of groups from 1 to 9 and the number of PCs included in computation from 2 to 5 (as an example, see Supplementary Material SM3, computed with the first 5 PCs, which account for about 60% of the total variance). Note that in the present scenario, a simpler K-means algorithm yields exactly the same results, as demonstrated in Supplementary Material SM4. However, Gaussian mixture models are generally a preferable choice due to their increased flexibility, especially regarding the covariance structures of the groups and the soft thresholding on group membership. In all of these cases, two groups optimally emerged here, both containing approximately the same number of individuals, i.e. 49 *vs* 58. They are strongly differentiated by PC1, but cover approximately the same range of values on PC2 (Fig. 4a). Unlike what is often observed in size-and-shape space (Klingenberg, 2016, 2022), here PC2 (and not PC1) is clearly associated with the centroid size. This is demonstrated by a
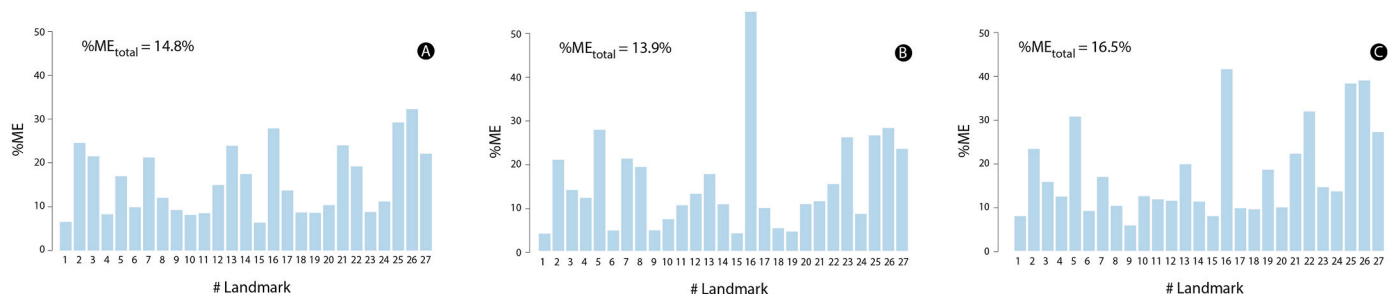

Fig. 2. Measurement error per landmark, expressed in percentage of total variation (%ME), for each of the three operators (A, B, and C). The total measurement error is also reported for each operator (%ME_Total).
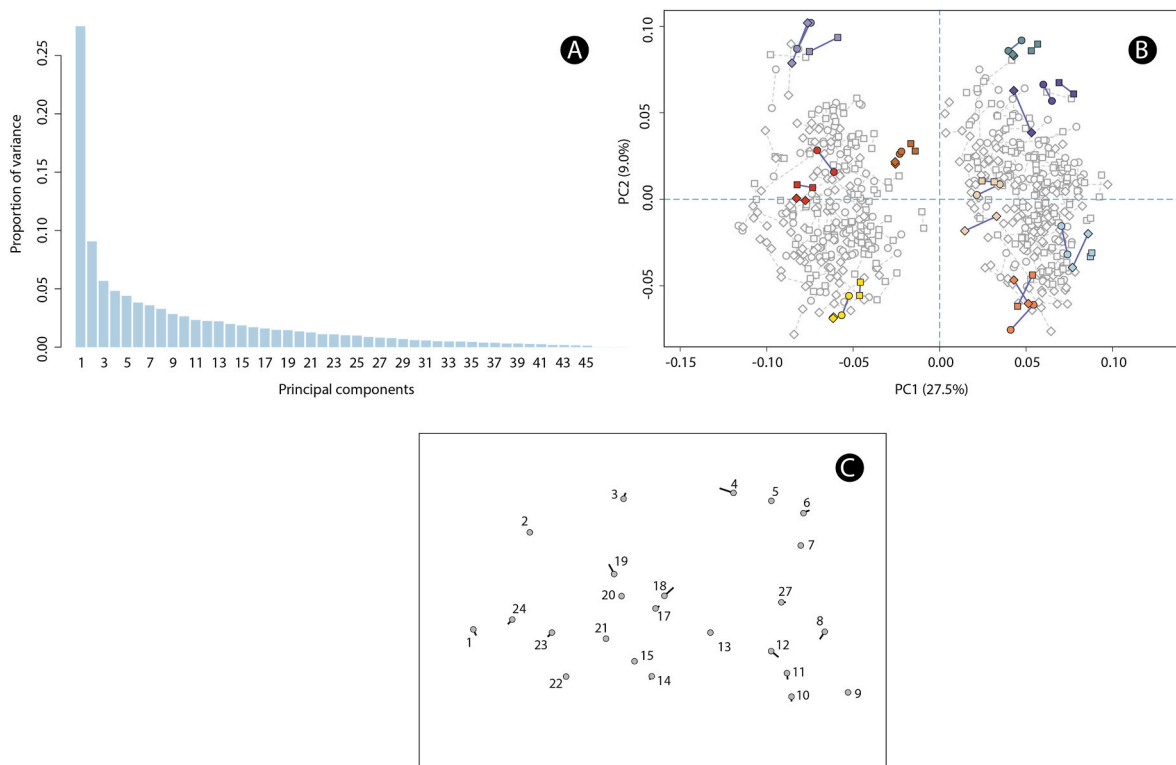
Fig. 3. (a) Scree plot for principal components and variance using the Boas coordinates of all replications as input. (b) Projection of the Boas coordinates on the first two principal components using a circle symbol for operator A, a square for operator B, a diamond for operator C, and a solid line linking the couples of duplicates; Nine specific individuals are highlighted and plotted using a different colour. (c) Vector change (intensity and main direction) of among-individual variation per landmark in relation to the mean shape. (For interpretation of the references to colour in this figure legend, the reader is referred to the Web version of this article.)

Table 1
Repeatability, expressed as *R*, and reproducibility, expressed as *R** (i.e., repeatability given that different operators have taken measurements).

Level	R	R*
Procrustes SS		
All operators	0.86	0.76
Operator A	0.87	
Operator B	0.86	
Operator C	0.88	
PC1	0.98	0.97
PC2	0.95	0.87
PC3	0.81	0.45

strong inverse correlation between PC2 and centroid size ($r = -0.84$, $p < 10^{-6}$; Fig. 4b). Besides this general observation, the two groups previously identified plot disjointedly in Fig. 4b, forming two linear regressions, for which differences were tested using an ANCOVA. No difference was observed in terms of slope values ($F_{1, 103} = 2.4$, $p = 0.12$), but y-intercepts were significantly different ($F_{1, 103} = 142.3$, $p < 10^{-6}$), indicating that PC2 could not only be driven by size, but also to some extent by shape. A slight but significant difference in centroid sizes was also noticed between the two groups ($t_{105} = -3.9$, $p = 2 \times 10^{-4}$). The angle between the allometric vector (represented by PC2) and the isometric vector is 34.7°, a value much smaller than the angle between two random vectors ($p = 2.2 \times 10^{-13}$). Form changes associated with increased PC2 values correspond to an overall change to a more compact shape, with a decrease in size (Fig. 4c). All vectors point roughly to the centroid, but not perfectly, nor with the same magnitude, underlining the slightly allometric nature of the shape changes.

To visually evaluate the differences in terms of shape (not size), two samples possessing approximately the same centroid size value (namely #10517953 and #10517978) were chosen from the middle of the two

groups. The Boas coordinates of their landmarks were plotted in the same diagram, together with their contours (Fig. 5). With such a representation, it becomes clear that beyond the remarkable homogeneity of shape, the most notable difference between the two groups is captured by landmarks #18 and #19, located under the belly of the animal. The shape of the ear is also probably discriminating, but no clear landmark could be recognized on its contour, except to some extent landmarks #4 and #5. In any case, attempting to define the exact shape of the entire ear would probably have been inefficient, as this part of the animal underwent significant finishing by the goldsmith. Unsurprisingly, landmarks #4, #18, and #19 were also those depicting the greatest among-individual variation within the entire population (Fig. 3c).

Interestingly, the projections in the 2D morphospace of the two distinct groups of shapes identified by geometric morphometrics do not overlap at all (Fig. 4a). This absence of overlap definitely rules out any gradual transition from one form to another that might be expected with progressive alteration of the moulds or imprints used to cast wax models, for example. Interpreting centroid size variation is not straightforward, as this feature, although carrying information, may lack meaning for the archaeologist. A more common variable would be the length of the objects, which could easily have been measured manually at submillimetre precision, for example with an electronic calliper. In this study, the distance between landmarks #1 and #9 is taken as a surrogate of total length. As expected, this distance appears to be positively correlated with centroid size ($r = 0.64$, $p < 10^{-6}$; cf. Supplementary material SM5). The range for this distance is about 1.5 mm for both groups, representing ~6% of the length of the longest individual in each group. To attribute such variation to presentation-related errors during the photography process would imply that some individuals would have been tilted by 20° relative to the horizontal plane, if all individuals were of the same size. This value is obviously far too high to be realistic, meaning that length variations, albeit small, exist in both groups. It is
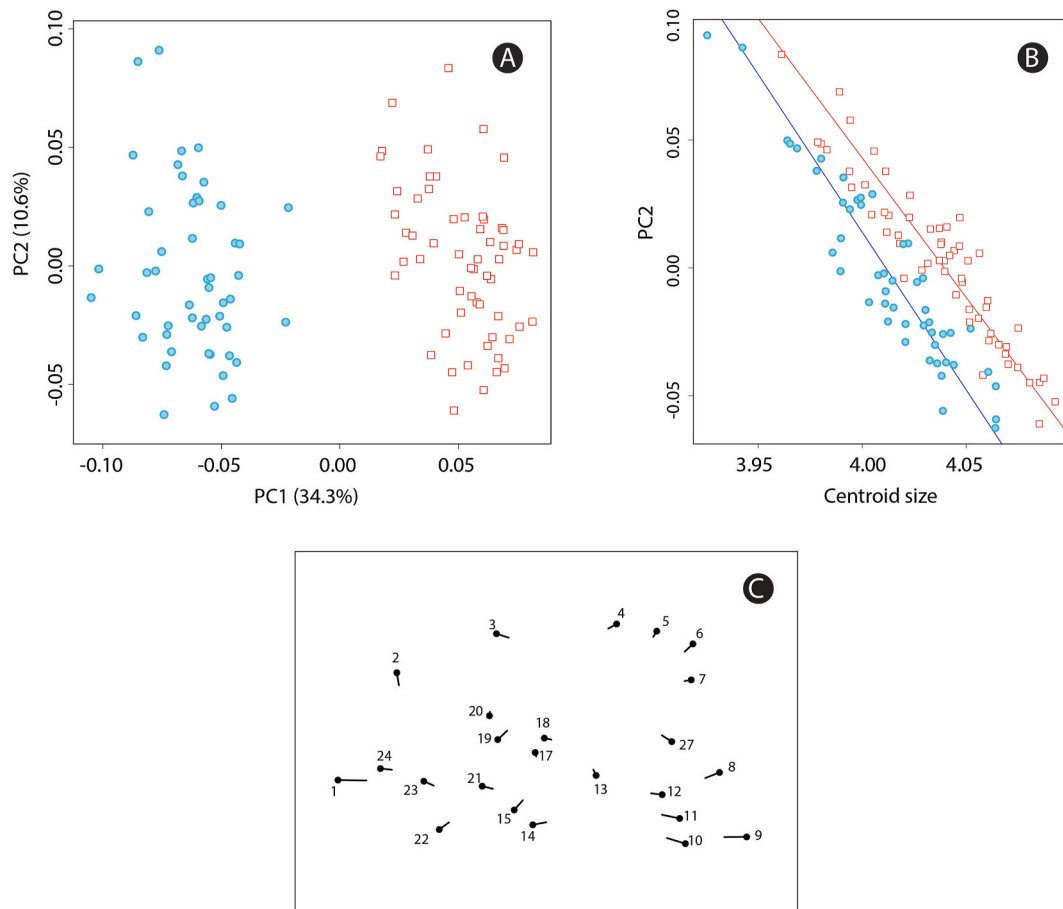
Fig. 4. (a) Projection of the averaged Boas coordinates on the first two principal components; in blue and red, the two shape groups identified. (b) PC2 vs centroid size; the two shape groups are also reported in blue and red, while the solid lines correspond to the linear regressions. (c) Form changes associated with positive increase along PC2 after scaling the eigenvectors. They are magnified to exemplify the shrinkage of the objects. (For interpretation of the references to colour in this figure legend, the reader is referred to the Web version of this article.)
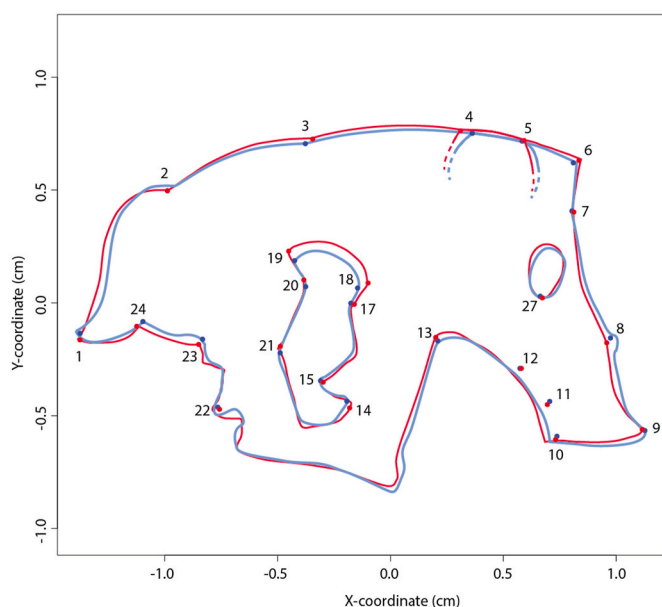

Fig. 5. Boas coordinates of the landmarks of the individuals #10517978 and #10517953, taken as representatives of blue and red shape groups. Both individuals are plotted on the same diagram together with their contours. (For interpretation of the references to colour in this figure legend, the reader is referred to the Web version of this article.)

worth noticing that once the centroid sizes of both groups are centred and gathered, the skewness of the distribution appears to be significantly negative (skewness = −0.45, z = −1.98, p = 0.024) with a d'Agostino skewness test (D'Agostino, 1970), suggesting asymmetry in the distribution with the tail towards lower values (see Supplementary Material SM6a). Taken separately, the skewness values of the two groups are negative: 0.60 and −0.34, but only the first value appears significantly negative: z = −1.81, p = 0.035 and z = −1.16, p = 0.12 (see Supplementary Material SM6b). This behaviour is fully compatible with a shrinkage effect of mould, wax model or gold, or a combination of these factors: most of the individuals would present a relatively steady size reduction in relation to the solid original models from which they derive (possibly made of wax), while a few others would be slightly more affected by shrinkage. It is common for biologists to describe how the morphology of living creatures changes with size, using allometric relationships where correlations are sought between shape variables and size (Klingenberg, 2016). Based on shape (i.e., the Procrustes tangent coordinates, instead of the Boas coordinates), the amount of linear correlation between the shape component and other factors (here size, grouping factor, and their interaction) is tested using a Procrustes ANOVA (Goodall, 1991). As anticipated, there is a significant effect of the grouping factor (i.e., the two groups differ in terms of shape), and this effect accounts for about 28% of the total shape variance (Table 2). The effect of size on shape is also significant (p = 0.003), indicating the presence of allometry; in other words, size change induces modifications in shape. However, this effect remains modest, as it represents only 1% of the total shape variance. Note that this finding was already identified

Table 2
Procrustes ANOVA computed to test the influence of different variables (size, grouping variable, and interaction of both) on shape variation.

	Df	SS	MS	R^2	F	Z	Pr (>F)
Size	1	0.0009	0.0009	0.014	2.2643	3.1207	0.003
Group	1	0.0181	0.0181	0.283	44.3316	4.9258	0.001
Size:Group	1	0.0004	0.0004	0.006	0.9109	−0.2107	0.591
Residuals	103	0.0420	0.0004	0.657			
Total	106	0.0640					

by the low value of the angle between PC2 and the isometric vector, suggesting only a small overall allometric effect. Interestingly, the allometric relationships are not significantly different in the two groups ($p = 0.591$), suggesting that the underlying retraction processes involved are the same. At this point, it is worth noting that almost two-thirds of the total shape variation can be considered as noise induced by casting and post-processing operations. Such a high value explains why the archaeological signal is not easy to perceive with the naked eye alone.

Archaeological implications. Considering the number of artefacts buried in the Arzhan-2 barrow, the use of gold and the high level of similarity achieved for serially produced goods, it is fair to assume that these artefacts were produced in the framework of a "retainer workshop" in Costin's (1991) classification. This type of production is described as a "large-scale operation with full-time artisans working for an elite patron or government institution within a segregated, highly specialized setting or facility" (Costin, 1991). However, several aspects of the organisation of production remain unclear. How many crafters were involved? How long did they work on the gold objects from the Arzhan-2 barrow? Were the crafters full-time specialists or did they work on a seasonal basis? Given the near-total absence of archaeological, iconographic, or written sources regarding early Scythian gold production (Armbruster, 2009; Lifantii, 2023), accurately answering these questions is very difficult. Yet indirect evidence from the investigation of goldsmiths' productions can provide further insight into their techniques and organisation. The observation of the objects found in the Arzhan-2 barrow shows that the artefacts can be grouped in five main technological categories: "cast products [...], simple sheet-metal products, pressed sheet-metal work, objects with granulation, filigree, or enamel, and precious metal inlays in iron" (Armbruster and Meyer, 2024). Such technological variability could indicate production involving different workshops.

Here, shape variations observed within the entire set cannot be explained by progressive changes in the morphology of the moulds. On the contrary, two distinct solid models (one very slightly smaller than the other) must have been involved in the production of this set of gold wild boars. The presence of one or more additional shape groups remains theoretically conceivable, but should more groups be present, their differences with the groups already recognized would be too subtle to be statistically identified. The two groups previously identified by authors working on this set were based solely on the number of eyelets on the reverse side and not on shape. From Fig. 5, which presents a representative item from each group, it might seem that distinguishing the two shape groups within the set of objects is actually a trivial task. However, it is important to remember that post-casting refinements carried out by the goldsmiths resulted in variations within each group, further blurring the overall picture. Even if shape variations had been identified among the plates composing the set, determining with the naked eye that the items are organized in clear groups would have been very difficult.

Taking as a hypothesis the scenario involving lost-wax casting proposed by Armbruster (2010, 2017), the size variation observed could be explained by the cumulative effect of several sources of shrinkage: (i) progressive shrinkage by drying of the mould used to produce wax replicas, (ii) variable shrinkage during wax cooling, producing models a few percent smaller than the cavity from which they derive, and (iii)

variable shrinkage of gold on solidification (which may easily reach 2% compared to the wax model; Hollenback and Skinner, 1946; Fusayama and Ogata, 1966). With the scenario proposed by Minasyan (2004), the bi-valve clay mould and the gold cast are both subject to shrinkage. Our approach cannot determine whether production involved wax models for casting, as proposed by Armbruster (2010), or "splash" casting and the use of bi-valve moulds, as suggested by Minasyan (2004). The process applied must nevertheless have been compatible with the size variations observed. It is worth mentioning that the partition of 49 versus 58 items belonging to each group is not statistically different from the 45% versus 55% distribution previously observed using eyelets ($\chi^2 = 0.004$, $p = 0.95$). If reverse pictures had been available, it would have been possible to see if the groups established based on shape and those based on the number of eyelets correspond. However, as the distribution observed is also not significantly different from a 50%–50% split ($\chi^2 = 0.75$, $p = 0.38$), this might suggest changes in mould or model, and thus in shape, either consecutive to an accidental defect that occurred at the middle of casting operations or, more probably, the existence of two distinct production lines, possibly running in parallel.

Geometric morphometrics therefore provides additional information regarding the organisation of the production of the gold wild boar figurines, as it allows for the identification of production batches, which are not based on chemical composition (Freestone et al., 2009; Martinón-Torres et al., 2014), but on subtle shape variations, matching different moulds or patterns. Combined with technological investigation or material analyses, this method produces a finely tuned model of the organisation of production, suggesting the existence of two production lines within the workshop where the wild boar figurines (also slightly affected by variable shrinkage) were produced. Although the results of this study of wild boar figurines do not quite have the far-reaching archaeological significance of the technological investigations carried out by Armbruster or Minasyan, they demonstrate the major contribution of geometric morphometrics to the better understanding of the organisation of serial productions. Indeed, in the absence of direct archaeological, written, or iconographic sources, our knowledge of ancient metallurgy relies mostly on indirect evidence from the investigation of artefacts. For instance, traces left by metalworkers are scarce throughout much of the Bronze and Early Iron Ages in Europe (Molloy and Mödlinger, 2020). Within this framework, typology, including classifications based on stylistic features, has been commonly used to identify groups of artefacts and discuss the economic aspects of their production and diffusion based on artefacts perceived as local or foreign (Costin, 1991, 2001; Olausson, 1988). However, this method is not suitable for studying seriality, which consists of one or more series of visually identical artefacts. Even more than other methods, such as material analyses, geometric morphometrics provides a way to investigate the organisation of serial production through the identification of batches based on very slight morphological variations.

4. Conclusion

Because the number of individuals here remains low enough to be processed by the naked eye, an expert could have reached the same conclusions as those exposed above, by measuring with high precision the total length of the individuals, and by focusing attention under the belly of the animal. Nonetheless, focusing on this specific region of

interest is only easy when one already knows where to look. Indeed, none of the previous authors working on this dataset had detected the presence of two distinct shapes with such subtle size differences. It is doubtful that a traditional approach would perform as well as geometric morphometrics in other instances of seriality, where a considerable number of very similar items are involved. The main advantage of the procedure described here is that the shape is mathematically defined, so that conclusions can be based on objective statistical inferences. Increasing the set of samples to be processed is therefore beneficial to the quality of the conclusions drawn, without introducing any further complexity in the analysis; it merely requires more time and effort to collect the landmarks (here, acquisition took two half-days per operator). As demonstrated in the present study, which deals with seriality reached by casting and thus moulds, the use of Boas coordinates is an asset, as they contain both shape and size information. The projection of individuals on to a common morphospace advantageously provides clearer visualization and interpretation for the problem at hand. It must however be mentioned that the procedure is not immune to problems, or at least difficulties. In a context of seriality, the dataset is homogeneous by nature, so measurement errors may drastically obscure the sought-after archaeological signal. Replicating acquisition in an appropriate way is advisable to evaluate the influence of this possibly deleterious source of variation. Even if presentation during the photographic session is carefully standardized, the position of the objects relative to the camera unavoidably leads to bias due to parallax. This is even truer for objects with substantial relief. A 3D approach remains possible, but it is known to be more time-consuming and demanding in terms of materials and computational resources. Despite such drawbacks, the use of these techniques should be encouraged because of their objectivity, especially when they are applied to the analysis of seriality. The workflow described can easily be adapted for nearly all archaeological sets produced in a serial manner. Nonetheless, researchers should be aware that geometric morphometrics, which focuses solely on form, may not address all inquiries. Combining it with other approaches such as microwear studies, chemical and isotopic analyses, and others may be necessary for a more comprehensive understanding of the production techniques employed by our ancestors.

CRediT authorship contribution statement

Fabrice Monna: Writing – original draft, Visualization, Validation, Supervision, Software, Project administration, Methodology, Investigation, Formal analysis, Data curation, Conceptualization. **Nicolas Navarro:** Writing – original draft, Visualization, Validation, Software, Resources, Methodology, Investigation, Formal analysis, Data curation, Conceptualization. **Yury Esin:** Writing – original draft, Methodology, Investigation, Conceptualization. **Tanguy Rolland:** Writing – original draft, Visualization, Validation, Software, Resources, Methodology, Investigation, Formal analysis, Data curation, Conceptualization. **Josef Wilczek:** Writing – original draft, Validation, Methodology, Investigation, Conceptualization. **Leonard Dumont:** Writing – original draft, Validation, Methodology, Investigation. **Jerome Magail:** Writing – original draft, Visualization, Validation, Methodology, Investigation, Conceptualization. **Anne-Caroline Allard:** Writing – original draft, Validation, Methodology. **Carmela Chateau-Smith:** Writing – original draft, Validation. **Chechena Mongush:** Data curation. **Saida Byrynnay:** Data curation. **Paul Alibert:** Writing – original draft, Visualization, Validation, Software, Resources, Methodology, Investigation, Formal analysis, Data curation, Conceptualization.

Declaration of competing interest

The authors have no competing interests to declare that are relevant to the content of this article.

Appendix A. Supplementary data

Supplementary data to this article can be found online at https://doi.org/10.1016/j.jas.2024.106021.

References

Adams, D.C., Rohlf, F.J., Slice, D.E., 2004. Geometric morphometrics: ten years of progress following the 'revolution'. Ital. J. Zool. 71, 5–16.

Adams, D.C., Rohlf, F.J., Slice, D.E., 2013. A field comes of age: geometric morphometrics in the 21st century. Hystrix 24, 7–14.

Adams, D.C., Otárola-Castillo, E., 2013. geomorph: an R package for the collection and analysis of geometric morphometric shape data. Methods Ecol. Evol. 4, 393–399.

Alexeyev, A., 2021. The gold of the Scythian kings in the Hermitage collection. State. Hermitage.Mus. 272.

Armbruster, B., 2000. Goldschmiedekunst und Bronzetechnik. Studien zum Metallhandwerk der Atlantischen Bronzezeit auf der Iberischen Halbinsel, Montagnac: M. Mergoil (Monographies Instrumentum 15, 232.

Armbruster, B., 2009. Gold technology of the ancient Scythians – gold from the kurgan Arzhan 2, Tuva. ArchéoSciences 33, 187–193.

Armbruster, B.R., 2010. Technologische Aspekte der Goldschmiedekunst aus Arzan 2. In: Chugunov, K.V., Parzinger, H., Nagler, A. (Eds.), Der Skythenzeitlichen Fürstenkurgan Arzan 2 in Tuva. Mainz, vol. 26. Verlag Philipp von Zabern, pp. 183–199. Archäologie in Eurasien. Bd.

Armbruster, B., 2017. Predmety yuvelirnogo iskusstva. In: Chugunov, K., Parzinger, H., Nagler, A. (Eds.), Tsarskiy Kurgan Skifskogo Vremeni Arzhan-2 V Tuve. Novosibirsk: Izdatelstvo IAE SB RASP, pp. 186–201 (in Russian).

Armbruster, B., Meyer, C., 2024. Gold artifacts from the early scythian princely tomb Arzhan2, Tuva — aesthetics, function, and technology. Arts 13 (2), 46. https://doi.org/10.3390/arts13020046.

Bailey, R.C., Byrnes, J., 1990. A new, old method for assessing measurement error in both univariate and multivariate morphometric studies. Syst. Zoot. 39, 124–130.

Bertemes, F., Furtwängler, A., 2008. Import and imitation in archaeology, langenweißbach: beier & beran. Schriften des Zentrums für Archäologie und Kulturgeschichte des Schwarzmeerraumes 11, 252.

Birch, T., 2018. Standardised manufacture of iron Age weaponry from southern Scandinavia: constructing and provenancing the havor lance. In: Dolfini, A., Crellin, R.J., Horn, C., Uckelmann, M. (Eds.), Prehistoric Warfare and Violence: Quantitative and Qualitative Approaches, Quantitative Methods in the Humanities and Social Sciences. Springer International Publishing, Cham, pp. 247–276. https://doi.org/10.1007/978-3-319-78828-9_12.

Birch, T., Martinón-Torres, M., 2019. Shape as a measure of weapon standardisation: from metric to geometric morphometric analysis of the Iron Age 'Havor' lance from Southern Scandinavia. J. Archaeol. Sci. 101, 34–51.

Bookstein, F.L., 1991. Morphometric Tools for Landmark Data: Geometry and Biology, 1991 – Mathematics – 435. Cambridge University Press.

Bookstein, F.L., 2021. A new method for landmark-based studies of the dynamic stability of growth, with implications for evolutionary analyses. Evol. Biol. 48, 428–457.

Bourdieu, P., 1977. Outline of a Theory of Practice. Cambirdge University Press.

Cardillo, M., 2010. Some applications of geometric morphometrics to archaeology. In: Ashraf, M.T., Elewa (Eds.), Morphometrics to Nonmorphometricians. (Lecture Notes in Earth Sciences). Springer, pp. 325–341.

Castiñeira-Latorre, C., Gascue, A., Cassini, G.H., Fernicola, J.C., 2024. Geometric morphometric analysis for the study of the design and function of the archaeological lithic projectile points of Uruguay. J. Archeol. Sci. Rep. 54, 104401.

Costin, C.L., 1991. Craft specialization: issues in defining, documenting, and explaining the organization of production. J. Archaeol. Method Theor 3, 1–56.

Costin, C.L., 2001. Craft production systems. In: Feinman, G.M., Price, T.D. (Eds.), Archaeology at the Millennium. A Sourcebook. Kluwer Academic/Plenum Publishers, New York, pp. 273–327.

Chugunov, K., Nagler, A., Parzinger, H., 2001. The golden grave from Arzhan. Minerva 13, 39–42.

Chugunov, K., Parzinger, H., Nagler, A., 2010. Mainz. Der Skythenzeitliche Fürstenkurgan Aržan 2 in Tuva, vol. 330. Verlag Philipp von Zabern, 289 Abb., 153 Taf. (Archäologie in Eurasien 26. Steppenvölker Eurasiens 3).

Chugunov, K., Parzinger, H., Nagler, A., 2017. Tsarskiy Kurgan Skifskogo Vremeni Arzhan-2 V Tuve. Izdatelstvo IAE SB RAS, Novosibirsk, p. 500 (in Russian).

D'Agostino, R.B., 1970. Transformation to normality of the null distribution of g1. Biometrika 57, 679–681.

Dempster, A., Laird, N., Rubin, D., 1977. Maximum likelihood from incomplete data via the EM algorithm. J. R. Stat. Soc. Series B 39, 1–38.

Dryden, I.L., Mardia, K.V., 1998. Statistical Analysis of Shape. John Wiley & Sons, Chichester, p. 376.

Fernández Navarro, V., Godinho, R.M., García Martínez, D., Garate Maidagan, D., 2024. Exploring the utility of Geometric Morphometrics to analyse prehistoric hand stencils. Sci. Rep. 14, 6336.

Fraley, C., Raftery, A.E., 2006. MCLUST version 3: an R package for normal mixture modeling and model-based clustering. Washington Univ. Seatle Dept. Of Statistics, p. 50. Technical Report No. 504.

Freestone, I., Price, J., Cartwright, C., 2009. The batch: its recognition and significance. Annales du 17eme Congres de l'Association Internationale pour l'Histoire du Verre 130–135.

Fruciano, C., 2016. Measurement error in geometric morphometrics. Dev. Gene. Evol. 226, 139–15.

Fu, Jiayi (Ed.), 2002. Zhongguo Wadang yishu. Shanghai: Shanghai shudian Chubanshe, p. 2 (in Chinese).

Fusayama, T., Ogata, K., 1966. Casting shrinkages of inlay golds of known composition. J. Prosthet. Dent 16, 1135–1143.

Gabillot, M., Monna, F., Alibert, P., Bohard, B., Camizuli, E., Dommergue, C.-H., Dumontet, A., Forel, B., Gerber, S., Jebrane, A., Laffont, R., Navarro, N., Specht, M., Chateau, C., 2017. Productions en série vers 1 500 avant notre ère. Des règles de fabrication au Bronze moyen entre la Manche et les Alpes à la lumière d'une étude morphométrique. In: Mordant, C., Wirth, S. (Eds.), Normes et variabilités au sein de la culture matérielle des sociétés de l'àge du Bronze, Paris, vol. 10. Société préhistorique française (Séances de la Société préhistorique française, pp. 19–31.

Gomes, D.G.E., 2022. Should I use fixed effects or random effects when I have fewer than five levels of a grouping factor in a mixed-effects model? PeerJ 10, e12794. https://doi.org/10.7717/peerj.12794.

Goodall, C.R., 1991. Procrustes methods in the statistical analysis of shape. J. R. Stat. Soc. Series B 53, 285–339.

Gower, J.C., 1975. Generalized procrustes analysis. Psychometrika 40, 33–51.

Hollenback, G.M., Skinner, E.W., 1946. Shrinkage during casting of gold and gold alloys. J. Am. Dent. Assoc. 33, 1391–1399.

Jeanty, A., Ros, J., Mureau, C., Dham, C., Lecomte, C., Bonhomme, V., Ivorra, S., Figueiral, I., Bouby, L., Evin, A., 2024. Identification of archaeological barley grains using geometric morphometrics and experimental charring. J. Archaeol. Sci. 105924.

Johannsen, J.W., 2015. Serial production and metal exchange in early bronze age scandinavia: smørumovre revisited. In: Suchowska-Ducke, P., Scott Reiter, S., Vankilde, H. (Eds.), Forging Identities. The Mobility of Culture in Bronze Age Europe, Oxford: BAR, S2772. International Series, pp. 73–83.

Klingenberg, C.P., 2013. Visualizations in geometric morphometrics: how to read and how to make graphs showing shape changes. Hystrix 24, 15–24.

Klingenberg, C.P., 2016. Size, shape, and form: concepts of allometry in geometric morphometrics. Dev. Gene. Evol. 226, 113–137.

Klingenberg, C.P., 2022. Methods for studying allometry in geometric morphometrics: a comparison of performance. Evol. Ecol. 36, 439–470.

Korol, G.G., Naumova, O.B., 2017. Khudozhestvennyy Metall U Kochevnikov (Tsentral'naya Aziya Rubezha I-II tys.). IA RAN, Moscow, p. 128 pp. (In Russian).

Kruta, V., 1971. Le Trésor de Duchcov dans les collections tchéquoslovaques. Severočeské Nakladatelství. Ústí nad Labem 109.

Kuijpers, M.H.G., 2017. The Bronze Age, a world of specialists? Metalworking from the perspective of skill and material specialization. Eur. J. Archaeol. 21, 550–571.

Leusch, V., Pernicka, E., Armbruster, B., 2014. Chalcolithic gold from varna - provenance, circulation, processing, and function. In: Meller, H., Risch, R., Pernicka, E. (Eds.), Metalle der Macht - Frühes Gold und Silber. Metals of power - Early gold and silver, Halle: Landesamt für Denkmalpflege und Archäologie Sachsen-Anhalt, pp. 165–182.

Lifantii, O., 2023. Looking at the evidence of local jewellery production in Scythia. Arts 12 (4), 151. https://doi.org/10.3390/arts12040151.

Liljequist, D., Elfving, B., Roaldsen, K.S., 2019. Intraclass correlation – a discussion and demonstration of basic features. PLoS One 14, e0219854.

Liu, Y., Tan, P., Yang, J., Ma, J., 2021. Social agency and prestige technology: serial production of gold appliqués in the early Iron Age north-west China and the Eurasian steppes. World Archaeol. 53, 741–761.

Lundström, F., MacLeod, N., Isaksson, S., Glykou, A., 2023. The harpoon stands yonder: shape variation and functional constraints in Mesolithic complex weapon points from the circum-Baltic Sea area. J. Archaeol. Sci. Rep. 51, 104148.

MacLeod, N., 2018. The quantitative assessment of archaeological artifact groups: beyond geometric morphometrics. Quat. Sci. Rev. 201, 319–348.

Martinón-Torres, M., Li, X.J., Bevan, A., Xia, Y., Zhao, K., Rehren, T., 2014. Fourty thousand arms for a single emperor: from chemical data to the labor organization behind the bronze arrows of the terracotta army. J. Archaeol. Method Theor 21, 534–562.

Mauss, M., 1936. Les techniques du corps. J. Psychol. 32 (3–4), 271–293.

McLachlan, G., Peel, D., 2000. Finite Mixture Models. John Wiley and Sons, New York, p. 456.

Minasyan, R., 2004. Sekrety skifskikh yuvelirov. In: Arzhan – Istochnik V Doline Tsarey. Arkheologicheskiye Otkrytiya V Tuve. Slaviya, St. Petersburg, pp. 40–44 (in Russian).

Minasyan, R., 2014. Metalworking in Ancient Times and the Middle Ages. State Hermitage Publishers, St. Petersburg, p. 472 (in Russian).

Minasyan, R., 2016. Ancient methods of production of the articles with embossed images. Moscow: Sobranie Scripta Antiqua 5, 279–292 (in Russian).

Mitteroecker, P., Gunz, P., Bernhard, M., Schaefer, K., Bookstein, F.L., 2004. Comparison of cranial ontogenetic trajectories among great apes and humans. J. Hum. Evol. 46, 679–698.

Mitteroecker, P., Schaefer, K., 2022. Thirty years of geometric morphometrics: achievements, challenges, and the ongoing quest for biological meaningfulness. Am. J. Biol. Anthropol. 178, 181–210.

Molloy, B., Mödlinger, M., 2020. The organisation and practice of metal smithing in later bronze age Europe. J. World PreHistory 33 (2), 169–232. https://doi.org/10.1007/s10963-020-09141-5.

Muñoz-Muñoz, F., Perpiñán, D., 2010. Measurement error in morphometric studies: comparison between manual and computerized methods. Ann. Zool. Fenn. 47, 46–56.

Nakagawa, S., Schielzeth, H., 2010. Repeatability for Gaussian and non-Gaussian data: a practical guide for biologists. Biol. Rev. 85, 935–956.

Okumura, M., Araujo, A.G.M., 2019. Archaeology, biology, and borrowing: a critical examination of Geometric Morphometrics in Archaeology. J. Archaeol. Sci. 101, 149–158.

Olausson, D., 1988. Dots on a Map. Thoughts about the way archaeologists study Prehistoric trade and exchange. In: Hardh, B., Larsson, L., Olausson, D., Petre, R. (Eds.), Trade and Exchange in Prehistory. Studies in Honour of Berta Stjernquist. Lunds Universitets Historiska Museum, Lund, pp. 15–24.

Parzinger, H., 2017. Burial mounds of Scythian elites in the Eurasian steppe: new discoveries. J. Br. Acad. 5, 331–355.

Pernicka, E., 2014. Possibilities and limitations of provenance studies of ancient silver and gold. In: Meller, H., Risch, R., Pernicka, E. (Eds.), Metalle der Macht - Frühes Gold und Silber. Metals of power - Early gold and silver, Halle: Landesamt für Denkmalpflege und Archäologie Sachsen-Anhalt, pp. 153–164.

Pineda, A., Courtenay, L.A., Téllez, E., Yravedra, J., 2023. An experimental approach to the analysis of altered cut marks in archaeological contexts from Geometrics Morphometrics. J. Archaeol. Sci. Rep 48, 103850.

Robinson, C., Terhune, C.E., 2017. Erreur dans la collecte de données morphométriques géométriques : combinaison de données provenant de plusieurs sources. Suis. J. Phys. Anthropol. 164, 62–75.

Roberts, P., 1997. Mass production of finewares in the roman world. In: Freestone, I., Gaimster, D. (Eds.), Pottery in the Making. British Museum Press, London, pp. 188–193.

Rohlf, F.J., Slice, D., 1990. Extensions of the Procrustes method for the optimal superimposition of landmarks. Syst. Zool. 39, 40–59.

Rohlf, F.J., Marcus, L.F., 1993. A revolution in morphometrics. Trends Ecol. Evol. 8, 129–132.

Rowlands, M.J., 1971. The archaeological interpretation of metalworking. World Archaeol. 3, 210–224.

Schaeffer, J., Benton, M.J., Rayfield, E.J., Stubbs, T.L., 2020. Morphological disparity in theropod jaws: comparing discrete characters and geometric morphometrics. Palaeontology 63, 283–299.

Sørensen, T.F., 2012. Original copies: seriality, similarity and the simulacrum in the Early Bronze Age. Dan. J. Archaeol 1, 45–61.

Stockhammer, P.W., 2017. The dawn of the copy in the bronze age. In: Stockhammer, C. Forberg/P.W. (Ed.), The Transformative Power of the Copy: A Transcultural and Interdisciplinary Approach. heiUP, Heidelberg, pp. 169–189.

Webley, L., Adams, S., 2016. Material genealogies: bronze moulds and their castings in later bronze age britain. Proc. Prehist. Soc. 82, 323–340.

Webster, M., Sheets, H.D., 2010. A practical introduction to landmark-based geometric morphometrics. Quant. Meth. Paleobiol. 16, 168–188.

Wilczek, J., Monna, F., Barral, P., Burlet, L., Chateau, C., Navarro, N., 2014. Morphometrics of Second Iron Age ceramicsestrengths, weaknesses, and comparison with traditional typology. J. Archaeol. Sci. 50, 39–50.

Wilczek, J., Monna, F., Gabillot, M., Navarro, N., Rusch, L., Chateau, C., 2015. Unsupervised model-based clustering for typological classification of Middle Bronze Age flanged axes. J. Archaeol. Sci. Rep 3, 381–391.

Wilson, L.A., Cardoso, H.F., Humphrey, L.T., 2011. On the reliability of a geometric morphometric approach to sex determination: a blind test of six criteria of the juvenile ilium. Forensic Sci. Int. 206, 35–42.

Yezerinac, S.M., Lougheed, S.C., Handford, P., 1992. Measurement error and morphometric studies: statistical power and observer experience. Syst. Biol. 41, 471–482.

Zaitseva, G.I., Chugunov, K.V., Dergachev, V.A., Nagler, A., Parzinger, G., Scott, E.M., Sementsov, A.A., Vasiliev, S., van Geel, B., van der Plicht, J., Lebedeva, L.M., 2004. Chronological studies of the arzhan-2 scythian monument in Tuva (Russia). Radiocarbon 46, 277–284.

Zaykov, V.V., Chugunov, K.V., Yuminov, A.M., Zaykova, Y.V., Kotlyarov, V.A., 2015. Composition of gold items from the Arzhan-2 burial complex (Tuva) and probable sources of the metal. In: Geoarcheology and Archeological Mineralogy–2015. Miass: Institute of Mineralogy, UB RAS, pp. 142–149 (In Russian).